Journal of Applied Microbiology ISSN 1364-5072

ORIGINAL ARTICLE

NanoSIMS 50 elucidation of the natural element composition in structures of cyanobacteria and their exposure to halogen compounds

T. Eybe[1], J.N. Audinot[2], T. Bohn[1], C. Guignard[1], H.N. Migeon[2] and L. Hoffmann[1]

1 Department of Environment and Agro-Biotechnologies, Centre de Recherche Public – Gabriel Lippmann, Belvaux, Luxembourg
2 Department of Material Sciences, Centre de Recherche Public – Gabriel Lippmann, Belvaux, Luxembourg

Keywords
bromine, cyanobacteria, deltamethrin, nanoscale, pesticide exposure, secondary ion mass spectrometry.

Correspondence
Torsten Bohn, CRP – Gabriel Lippmann, 41, Rue du Brill, L-4422 Belvaux, Luxembourg.
E-mail: bohn@lippmann.lu

2007/1766: received 5 November 2007, revised 7 April 2008 and accepted 10 April 2008

doi:10.1111/j.1365-2672.2008.03870.x

Abstract

Aims: NanoSIMS (secondary ion mass spectrometry) is a powerful technique for mapping the elemental composition of a variety of small-scale samples (e.g. in Material Research, Cosmochemistry and Geology). However, its analytical features are making it also valuable to address biological questions. We demonstrate the ability of the NanoSIMS 50 to map elements at subcellular lateral resolution (approx. 50 nm) within cyanobacteria (*Anabaena* sp. and *Cylindrospermum alatosporum*) and its feasibility to investigate the uptake of bromine-containing substances (NaBr and deltamethrin).

Methods and Results: Elemental maps of O, N, P and S were obtained from semi-thin sections of different cell types (chemically fixed and resin-embedded heterocysts, akinetes and vegetative cells). NanoSIMS enabled the detection of various characteristic cell sub-structures and inclusions. A homogenous bromine distribution was detected following NaBr and deltamethrin exposure, at Br-concentrations of 0·05, 0·5 (NaBr) and 0·0025 mmol l^{-1} (deltamethrin).

Conclusions: NanoSIMS allowed study of the mapping of common elements in cyanobacterial cells and the uptake of NaBr and deltamethrin.

Significance and Impact of the Study: These results highlight the potential usefulness of NanoSIMS analysis for tracking elements within cell structures at the nanoscale and the ability to detect marker elements of xenobiotic compounds within exposed organisms.

Introduction

There is an increasing interest in using secondary ion mass spectrometry (SIMS) in biology and life sciences. Recent investigations include mapping and quantification of chemical compositions, such as detecting organic compounds (Hallegot *et al.* 2004), halogens (Guerquin-Kern *et al.* 2005; Hallegot *et al.* 2006) metals (Audinot *et al.* 2004; Marxer *et al.* 2005; Quintana *et al.* 2006; Krein *et al.* 2007), and isotopic ratio measurements (Audinot *et al.* 2006; Lechene *et al.* 2006; Clode *et al.* 2007; Popa *et al.* 2007) in cell structures or tissues. Despite the increasing number of applications, there still remains a paucity in making full use of NanoSIMS technology for biological environmental samples, such as for studying the fate of nonlabelled xenobiotic compounds or heavy metals in animal, plant and bacterial cells. This is at least partly attributed to challenges in sample preparation and location of the region of interest to be measured (Herrmann *et al.* 2007).

The high sensitivity, high lateral resolution (approx. 50 nm using Cs^+), and high transmission at high mass resolution (approx. 4000) for secondary ions make the NanoSIMS 50 a powerful tool for investigating elemental composition of microbiological samples. Distribution maps of several elements and their isotopes can be obtained simultaneously from the same sample area by raster scanning the sample surface with the primary ion beam, in conjunction with using a multi-detector. Thus, the main advantage of this technology is the ability to observe the distribution of a variety of elements at their original cell location. However, as biological samples have

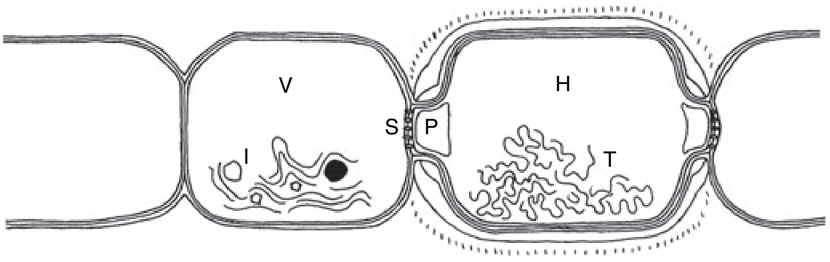

Figure 1 Schematic overview of filamentous cyanobacteria. H, heterocyst; I, inclusions, such as cyanophycin, polyphosphate, carboxysomes; P, pore channel; S, septum with microplasmodesmata; T, thylakoid membranes; V, vegetative cell. Outer layers of heterocyst: plasma membrane, murein, outer membrane, additional envelope (containing glycolipid layer, polysaccharide layer and fibrous layer).

to be vacuum compatible for measurement with the NanoSIMS 50, sample preparation, such as chemical or cryogen fixation and dehydration, remains a crucial part of using this technique. Depending on the specific method employed, changes in the elemental composition of samples have been reported. For example, chemical fixation and dehydration with organic solvents resulted in ion shifts and changed structural analysis. On the other hand, cryogen fixation can be time consuming and requires expensive and sophisticated instrumentation (Edelmann 2002).

Cyanobacteria (Fig. 1) represent naturally widespread prokaryotes which have been successfully used as a biological indicator for different purposes (Parikh *et al.* 2006; Jancan *et al.* 2007). Cyanobacteria play an important role in the carbon and nitrogen cycle and appear in many different environments from Arctic to Antarctic waters, soils, hot springs and crop fields (Madigan *et al.* 2000). Under normal conditions, cyanobacteria are characterized by single cells or by filaments of vegetative cells. Depending on nutrient supplies, vegetative cells of a number of species can differentiate into akinetes (spores) or heterocysts (Wolk 1996).

In the present study, we investigated the usefulness of NanoSIMS to determine the distribution of the naturally abundant elements O, N, P and S in different cyanobacteria cell types. In addition, the distribution of bromine following the exposure of cyanobacteria to nonisotopically enriched NaBr and deltamethrin (Fig. 2), a bromine containing pesticide, were studied. Deltamethrin was included to determine the ability of the NanoSIMS 50 to map this xenobiotic compound within the cells. Measurements were carried out following chemically fixed and resin embedded cells.

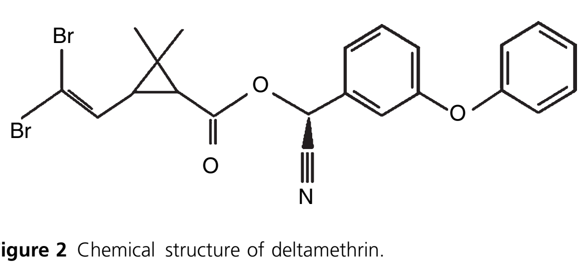

Figure 2 Chemical structure of deltamethrin.

Methods

Sample preparation

The cyanobacteria *Anabaena* sp. and *Cylindrospermum alatosporum* [culture collection of algae (SAG), University of Göttingen, Germany] were grown in culture bottles (Easy flask, 25 Filt Delta, VWR International GmbH, Darmstadt, Germany) at 22°C in 30 ml BG11$_0$ medium as described by Rippka (1988), containing no nitrogen sources. Unless otherwise stated, all chemicals were obtained from Sigma-Aldrich (Seelze, Germany) and were of analytical grade or superior.

Cells were harvested by centrifugation (Sanyo/MSE Harrier 18/80 Refrigerated, Jepson Bolton & Co Ltd., Watford, UK) for 1–2 min at 100 ***g*** at room temperature, and washed with 0·5 ml phosphate-buffered saline (PBS, 0·1 mol l^{-1}). The cyanobacteria were embedded in 1% agar and cut into small cubes (edge length of 1–2 mm), a method allowing for embedding without further centrifugation.

The first fixation was done with 5% glutaraldehyde in PBS (0·1 mol l^{-1}) overnight. Glutaraldehyde was removed and cells were washed in pure PBS. The cyanobacteria were then postfixed with osmium tetroxide (0·2% in H_2O) overnight for 16 h. After an additional washing step with PBS (0·1 mol l^{-1}) and dehydration with five increasing acetone concentrations (30%, 50%, 70%, 90% and 100% acetone), the cyanobacteria were embedded in epoxy resin (Epon 812 substitute). The samples were cut to 500-nm semi-thin sections (Leica ultracut UCT, Le Pecq Cedex, France) and placed on gold-foil-coated wafers (Goodfellow, Cambridgeshire, UK) and silicon wafers (Siltronix, Archamps, France) for NanoSIMS analysis. The samples were stored in plastic boxes at room

Table 1 Exposure* of *Anabaena* sp. with added NaBr and deltamethrin

	Control	NaBr	Deltamethrin
Final concentrations of added Br (μmol ml^{-1})	–	0·005	0·00025
		0·05	0·0025
		0·5	0·005
		n.a.†	0·05

*Exposure time 5 days, temperature of 21·9°C, BG11$_0$ medium.
†n.a., not applicable, i.e. was not carried out.

temperature in the dark. For each cell type and exposition experiment, a minimum of five samples were measured.

Halogen salt and pesticide exposure experiment

Cells of *Anabaena* sp. were grown in BG11$_0$ medium as previously described for sample preparation in this paper. NaBr (Merck, Darmstadt, Germany) and the pesticide deltamethrin, dissolved in ethanol, were added to result in final concentrations as outlined in Table 1. The cells were prepared for NanoSIMS 50 analysis as described earlier. Cells without any special exposure (control) were prepared in parallel in the same way.

NanoSIMS 50 parameters

The SIMS observations were performed with a NanoSIMS 50 (Cameca, Courbevoie, France) using a Cs$^+$ primary source (8 keV), rasterizing the surface of the sample (−8 keV) with a raster between 8 × 8 μm and 16 × 16 μm to generate secondary negative ions. The energy of the impact of the primary beam was 16 keV. The probe working diameter was in the range 80–100 nm, with an intensity range of 1·0–0·8 pA. The masses studied simultaneously in multicollection mode were: $^{16}O^-$ (m = 15·99491), $^{12}C^{14}N^-$ (m = 26·00307), $^{31}P^-$ (m = 30·97376), $^{32}S^-$ (m = 31·97207) and $^{81}Br^-$ (m = 80·91629). Images were recorded in a pixel format of 256 × 256 image points with a counting time of 20 ms per pixel. Mass resolution ($M/\Delta M$) was above 4000 and mass calibration of Br was achieved using standard references (NaBr salt).

Results

Natural abundant element composition

Figures 3–5 show different simultaneously recorded element images from various cells of *C. alatosporum* and *Anabaena* sp. With a high lateral resolution of approx. 50 nm, the NanoSIMS 50 illustrated the elemental distribution of oxygen, nitrogen (measured as CN$^-$), phosphorus and sulfur in different types and structures of cells, even in the comparatively small vegetative cells of approximately 3–5 μm.

Relatively small structures in the cells were clearly detected, such as pore channel (approx. 400 nm) and additional envelope of the heterocyst (thickness of approx. 100 nm) from *C. alatosporum* (Fig. 3). The concentration of the detected elements inside the heterocyst's additional envelope was higher compared with the cytoplasm. Furthermore, the cytoplasm was visible with

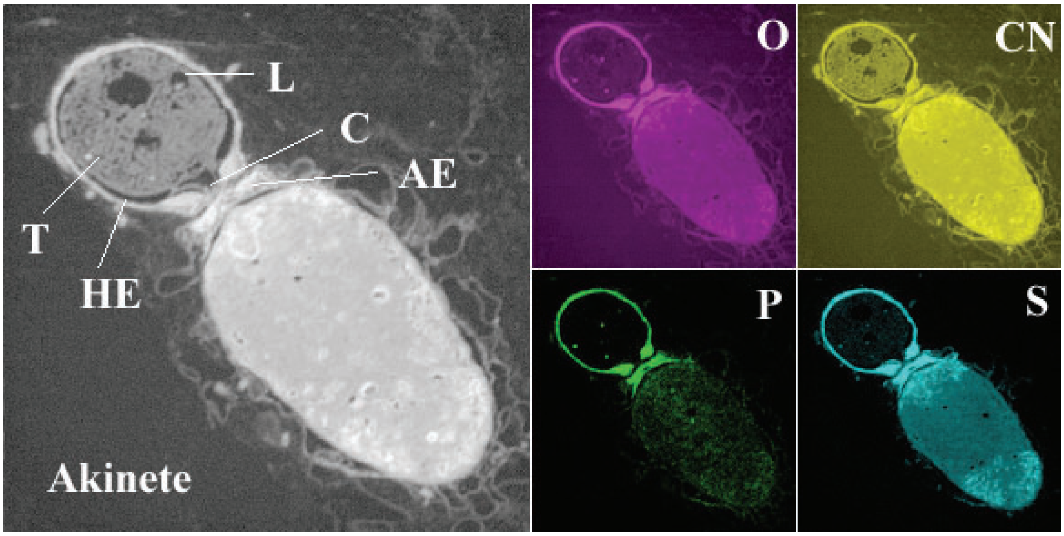

Figure 3 Heterocyst and akinete of *Cylindrospermum alatosporum*. Left: overview. AE, remains of akinete additional envelope; HE, additional heterocyst envelope; L, lipid body or gap in the thylakoid membranes; P, pore channel; T, cytoplasm with thylakoid membranes. Right: NanoSIMS 50 images of different elements. Raster size 16 × 16 μm. Increasing brightness indicates stronger secondary ion intensities within the image.

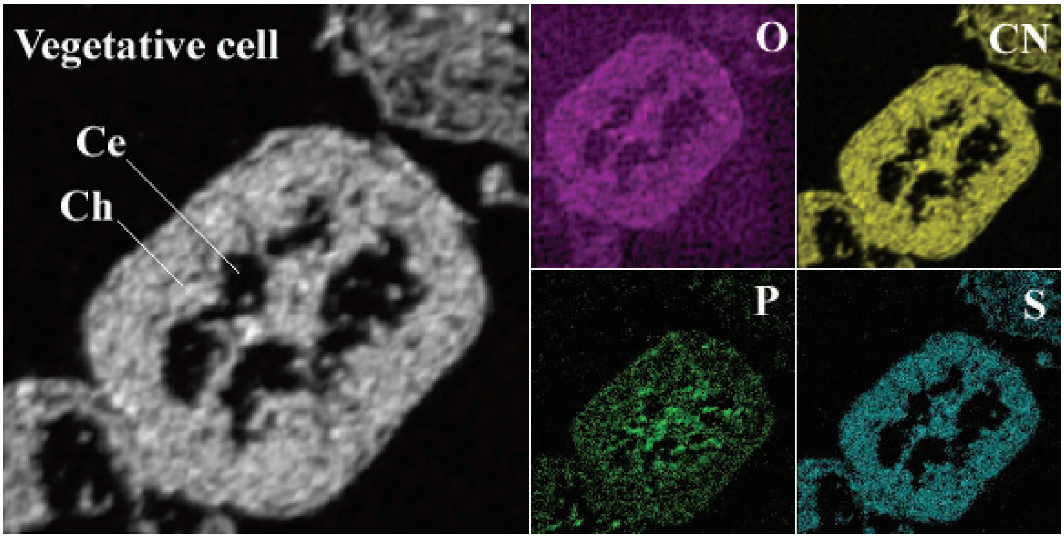

Figure 4 Vegetative cell of *Anabaena* sp. Left: overview. Ce, centroplasm; Ch, chromatoplasm. Right: NanoSIMS 50 images of different elements. Raster size 8 × 8 μm. Increasing brightness indicates stronger secondary ion intensities within the image.

its approx. 40-nm thick thylakoid membranes and gaps between the thylakoid membranes (300–500 nm) that may indicate lipid bodies.

The NanoSIMS 50 was also feasible for detecting the separation inside the vegetative cells of *Anabaena* sp. (Fig. 4) into chromatoplasm (location of thylakoids) and centroplasm (location of DNA, low thylakoid content), whereas vegetative cells of *C. alatosporum* (Fig. 5a) showed no differentiation. A higher phosphorus signal in the area of the centroplasm of the *Anabaena* sp. vegetative cell potentially indicated DNA. In the vegetative cells of *C. alatosporum* (Fig. 5a), a variety of cellular inclusions were visible (bright spots) for different elements, in addition to the cell wall (bright line) that separated the cells of the filament. A region of higher sulfur content indicated a high protein content. Cellular inclusions, most likely being polyphosphates, could also be detected.

Figure 5b shows an image of an *Anabaena* sp. akinete, with easily identifiable cellular structures, such as the additional envelope and the cell wall layer. In comparison with an akinete of *C. alatosporum* (Fig. 5c), where the cytoplasm seemed to be nearly homogenous, large cellular inclusions (200–300 nm) in *Anabaena* sp. could be documented, which may indicate cyanophycin, because of their high nitrogen content. A higher sulfur concentration in the *C. alatosporum* akinete cytoplasm in Fig. 3 at the poles near the adjacent cells suggests also the presence of proteins.

Exposure to halogen salts and deltamethrin

Figure 6 shows NanoSIMS 50 images of the exposure experiments of *Anabaena* sp. with halogen-containing compounds. The highest amount of Br was found following exposure of 0·5 μmol ml^{-1}, followed by 0·05 μmol ml^{-1} NaBr and 0·0025 μmol ml^{-1} Br from deltamethrin. Deltamethrin concentrations of 0·005 μmol ml^{-1} and above caused cell death after 1 day of exposure, while lower concentrations of NaBr and deltamethrin could not be differentiated visually from the negative control samples. Br from NaBr and deltamethrin could be detected in all exposed cell types and did not indicate any preferred enrichment in any cell types or in special cell structures.

Discussion

In this study, we tested the applicability of the NanoSIMS 50 to map the structure and the natural abundant element composition within chemically fixed and resin-embedded cyanobacteria. This method differs from other bacteria studies with NanoSIMS analysis in which the surfaces of cells were investigated after drying cyanobacteria on sample wafers (Lechene *et al.* 2006; Popa *et al.* 2007). Cyanobacterial cells possess a diversity of particular structures and are attributed to their small size (diameter of approx. 3–10 μm) and suitable models for implementing NanoSIMS 50 techniques to measure the natural elemental composition at the nanoscale. The present results demonstrate the high lateral resolution of the NanoSIMS 50 and the ability of the chemical fixation technique to investigate and map cell structures of different cyanobacterial cell types for abundant and physiologically important elements, including oxygen, nitrogen, phosphorus and sulfur. Small structures, such as pore channels, cell walls and thylakoid membranes, could be differentiated. Furthermore, cellular uptake of Br from NaBr and deltamethrin could be monitored. To our knowledge, this is the first report applying the NanoSIMS 50 for xenobiotic exposure studies in living organisms.

According to Peteranderl and Lechene (2004), biological tissues are typically composed of approximately 60% carbon and 11% nitrogen. Although nitrogen had to be detected as cyanide (CN^-) as it does not produce secondary ions, it was possible to show the general cell morphology by imaging the CN^- distribution. Prevalent elements, such as oxygen and hydrogen, are part of sugars, proteins and lipids. Phosphorus as part of nucleic acids can indicate the position of DNA and RNA. Sulfur mainly indicates the protein distribution, as the disulfide bridges in the proteins are responsible for their three-dimensional protein structure. Based on this elemental mapping, the NanoSIMS 50 was able to detect a variety of structures hypothesised to reflect polyphosphate (P and O), lipid bodies (no P, no CN, no S detectable), and cyanophycin granules (high CN) and DNA (P), being in line with earlier observations (Madigan *et al.* 2000). In the present study, we revealed that the additional envelopes from heterocysts and akinetes likewise contained the elements O, C, N, P and S. These results agree with former findings (Dunn and Wolk 1970; Cardemil and Wolk 1976, 1979) postulating that both envelopes, from heterocysts and akinetes of *Anabaena cylindrica*, contain amino compounds, lipids and carbohydrate, such as glucose, mannose, galactose and xylose.

Compared with the NanoSIMS 50, other analytical methods, such as inductively coupled plasma mass spectrometry (ICP-MS), ICP-AES (atomic emission spectrometry) or AAS (atomic absorption spectrometry) can also detect the chemical constitution of biological samples, with a sensitivity range of ppb to ppt (Ammann 2007). The limit of detection of the SIMS technique is typically in the ppb to ppm range for smaller volumes (Clerc *et al.* 1997). With a pulverized volume of the present samples of around 50 to 80-nm diameter and 1- to 2-nm depth, it is possible to detect the small amount of approx. 300 carbon atoms (Slodzian *et al.* 1990). However, the aforementioned analytical methods have the limitation that samples typically need a relatively long sequence of

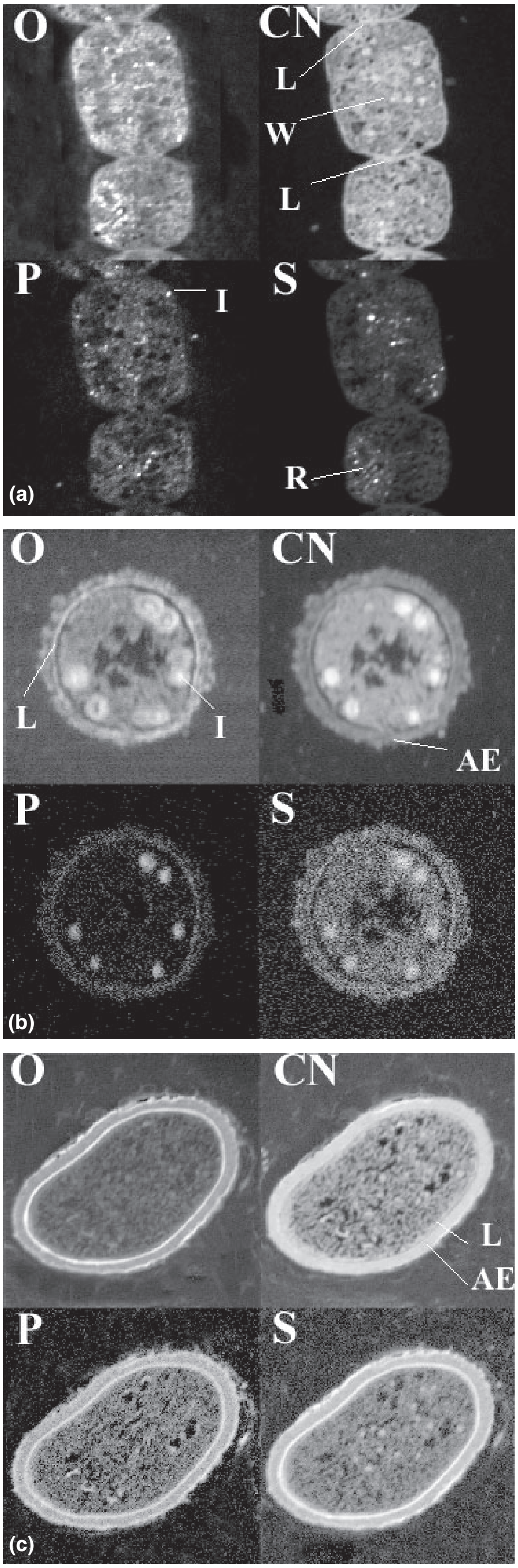

Figure 5 (a): O, CN, P and S elemental maps. Vegetative cells of *Cylindrospermum alatosporum*. Raster size 8 × 8 μm. R, region of higher sulfur content. Increasing brightness indicates stronger secondary ion intensities within the image. (b) O, CN, P and S elemental maps. Akinete of *Anabaena* sp. Raster size 8 × 8 μm. Increasing brightness indicates stronger secondary ion intensities within the image. (c) O, CN, P and S elemental maps. Akinete of *C. alatosporum*. Raster size 11 × 11 μm. Increasing brightness indicates stronger secondary ion intensities within the image. I, inclusion; L, cell wall layer; W, cytoplasm without separation in centroplasm and chromatoplasm; AE, additional akinete envelope.

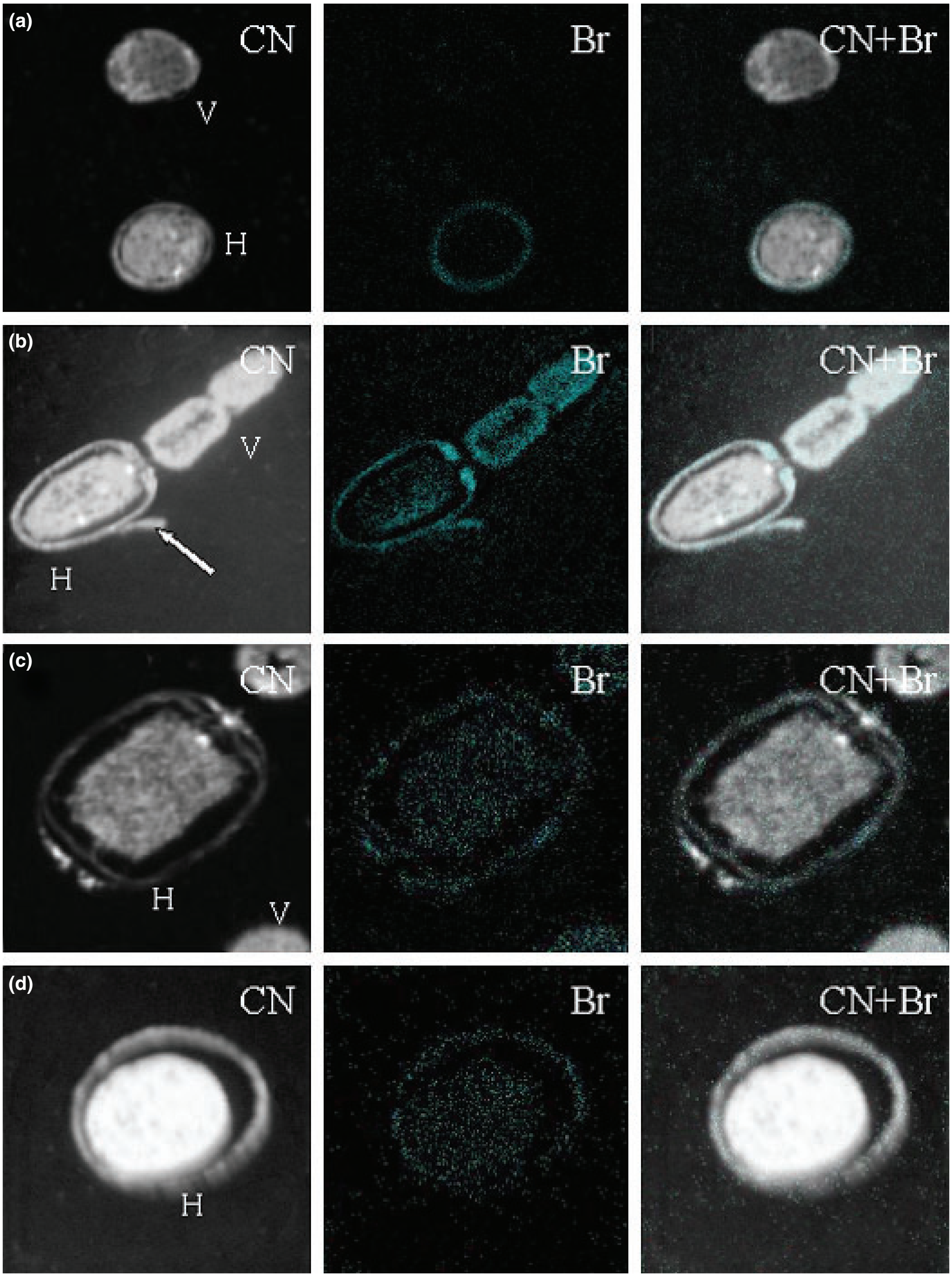

Figure 6 Exposure of *Anabaena* sp. (a) Control, raster size 15 × 15 μm; (b) NaBr: 0·5 μmol ml^{-1} Br, raster size 15 × 15 μm; (c) NaBr: 0·05 μmol ml^{-1} Br, raster size 10 × 10 μm; (d) deltamethrin: 0·0025 μmol ml^{-1} Br, raster size 8 × 8 μm. H, heterocyst; V, vegetative cell; white arrow, epibiontic rod-shaped bacteria on the surface of a heterocyst. In the right column, the CN + Br images show that bromine overlaps with the cyanobacteria structures.

preparative steps and tissues have to be digested and minerals to be dissolved (Buldini *et al.* 2002; Yang 2007). Thus, a prediction about the original location of the detected elements within the cell structures is not possible. NanoSIMS in combination with the chemical embedding procedure possesses the advantage to virtually 'look' directly into cells. It can therefore map the elemental/isotopic distribution of the different cell structures, revealing both information about the morphology and the elemental composition. Microscopic techniques, such as fluorescence microscopy using fluorescent tags have also been used to detect elemental composition at subcellular scales; however, these tags did often change physical and chemical properties of the labelled component (Marxer *et al.* 2005). Another microscopic method is X-ray microanalysis, scanning a sample with an intense electron beam to generate a high-elemental resolution map. This technique has already been used to characterize bacterial cells (Norland *et al.* 1995) and spores (Stewart *et al.* 1981). However, the detection limit is relatively high (1%), and measuring isotopic composition is not possible. Even in comparison with other SIMS techniques, the NanoSIMS 50 exhibits additional advantages. Usually, NanoSIMS is designed to work in dynamic SIMS mode. Its parallel detection mode allows continuous sputtering and therefore considerably higher secondary ion yields and shorter acquisition times. In addition, the high lateral resolution of 50 nm makes it well suited for biological samples on the small scale (Marino *et al.* 2006).

Cyanobacteria have been used as test organisms for xenobiotic compounds owing to their broad occurrence and ease of cultivation. We tested the use of *Anabaena* sp. in combination with the NanoSIMS 50 to detect the uptake of a frequently used pesticide. Pyrethroid insecticide use, such as deltamethrin, is steadily increasing for agricultural purposes, commercial pest control and residential consumer use. Relatively little is known about the toxicity of sediment-associated pyrethroid residues to aquatic organisms (Amweg *et al.* 2005). Deltamethrin exhibits a nonpolar nature and can therefore accumulate in lipid tissues of living organisms. Bio-concentration factors (BCF) found in fish ranged from 360 to 6000 (Laskowski 1999). In the present study, deltamethrin showed the same detectable enrichment in cyanobacteria following a 20-fold lower exposure concentration compared with NaBr, probably because of a higher bioconcentration factor owing to its nonpolar nature (CambridgeSoft Corporation Internet 2007). This would indicate either increased absorption or persistence in the cells. To accumulate inside the cell, substances have to pass the cell membrane. The lipid layer can only be passed by diffusion by lipophilic substances, whereas ions typically need specific transport mechanisms involving membrane proteins (Wehner and Gehring 1995). It could therefore be speculated that bromine in form of NaBr was absorbed preferably via transport through membrane proteins, whereas deltamethrin was absorbed by passive diffusion.

Exposed to pesticides, cyanobacteria can show different responses. Deltamethrin is known to negatively affect cyanobacterial mass (Hutber *et al.* 1979; Mallison and Cannon 1984). Pyrethroid insecticides have caused a reduction in the chlorophyll-a content of *Anabaena doliolum* (Widenfalk *et al.* 2004), and deltamethrin-like pyrethroids have shown to bind to lipid bilayers (Michelangeli *et al.* 1990), demonstrating that deltamethrin can reach the thylakoid membrane rich cytoplasm in cyanobacteria. In our present study, we observed a rather homogenous distribution of Br from deltamethrin within the cyanobacterial cells, being in line with the hypothesis that deltamethrin binds to the ubiquitously present thylakoid membranes within the cytosol. However, a similar distribution was found by exposing cyanobacteria to NaBr. It is possible that a higher resolution than the achieved 50 nm is required to reveal differences in the distribution of bromine from these two compounds.

Although it has been reported that chemical embedding may lead to ion shifts, water shifts, and structural changes of the respective samples (Edelmann 2002; Warley 2006) and it has been recommended to use cryogenic methods for studies involving diffusible ions or small molecules (McMahon *et al.* 2006), it was possible in the present study to detect bromine inside the chemically fixed and resin-embedded cells following exposure to NaBr and deltamethrin. Bromine was clearly detected within the cell structures and not within the surrounding resin, suggesting that it was bound, at least to a large extent, inside the cells. In addition, the visual integrity of subcellular structures of the cyanobacteria confirmed that no major structural changes occurred. It was thus assumed that the detected elements associated with the structures and inclusions within the cyanobacteria were not in a soluble form (ions) but remained at their cell structures. Furthermore, the suitability of chemical embedding procedures for compositional biological elements, such as nitrogen, phosphorus and sulphur, was already demonstrated by Quintana *et al.* (2007) and Clode *et al.* (2007). Thus, these findings make the chemical embedding procedure apparently useful for studies of cell structure composition and xenobiotic recovery with NanoSIMS techniques. However, additional studies are needed to fully optimize this cost-efficient and time-saving technique of chemical fixation.

In addition to the exposed cells, the control sample also showed a low Br signal inside the additional cell envelope of the heterocysts from *Anabaena* sp. (Fig. 6), indicating its natural occurrence. It has been assumed that Br is essential for a number of organisms as reported for Rhodophyceae (Marshall *et al.* 2003; Carter-Franklin and Butler 2004), mollusc pigments (Rutherford online Internet 2007) and human serum (Cuenca *et al.* 1988). A comparison with a number of control samples is therefore indispensable.

In conclusion, the present investigations demonstrate that NanoSIMS can be a valuable tool to investigate the elemental composition of cell structures and inclusions at the nano scale. Furthermore, it allows for determining the biological fate following halogen exposure from different origins inside the cells. These results highlight that NanoSIMS 50 could be an attractive analytical method in cell biology and ecotoxicology to study the fate of pollutants upon uptake by living organisms. Future studies employing the NanoSIMS 50 as a tool for uptake and analysis of biologically relevant compounds in biological structures are merited, and efforts for further optimization towards quantitative interpretation and improved lateral resolution are desired.

Acknowledgements

This work was realized in the framework of the project 'Nano environment', supported by the Fonds National de la Recherche (FNR, Luxembourg) within the 'Innovative Materials and Nanotechnology' programme.

References

Ammann, A.A. (2007) Inductively coupled plasma mass spectrometry (ICP MS): a versatile tool. *J Mass Spectrom* **42**, 419–427.

Amweg, E.L., Weston, D.P., Ureda, N.M., Boxall, A. and Long, C. (2005) Use and toxicity of pyrethroid pesticides in the Central Valley, California, USA. *Environ Toxicol Chem* **24**, 966–972.

Audinot, J.N., Schneider, S., Yegles, M., Hallegot, P., Wennig, R. and Migeon, H.N. (2004) Imaging of arsenic traces in human hair by nano-SIMS 50. *Appl Surf Sci* **23**, 1–232.

Audinot, J.N., Guignard, C., Migeon, H.N. and Hoffmann, L. (2006) Study of the mechanism of diatom cell division by means of 29Si isotope tracing. *Appl Surf Sci* **252**, 6813–6815.

Buldini, P.L., Ricci, L. and Sharma, J.L. (2002) Recent applications of sample preparation techniques in food analysis. *J Chromatogr A* **975**, 47–70.

CambridgeSoft Corporation. *Deltamethrin*. 2004. Internet: http://chemfinder.cambridesoft.com (accessed July 3, 2007).

Cardemil, L. and Wolk, C.P. (1976) The polysaccharides from heterocyst and spore envelopes of a blue-green alga. Methylation analysis and structure of the backbones. *J Biol Chem* **251**, 2967–2975.

Cardemil, L. and Wolk, C.P. (1979) The polysaccharides from heterocyst and spore envelopes of a blue-green alga. Structure of the basic repeating unit. *J Biol Chem* **254**, 736–741.

Carter-Franklin, J.N. and Butler, A. (2004) Vanadium bromoperoxidase-catalyzed biosynthesis of halogenated marine natural products. *J Am Chem Soc* **126**, 15060–15066.

Clerc, J., Fourre, C. and Fragu, P. (1997) SIMS microscopy: methodology, problems and perspectives in mapping drugs and nuclear medicine compounds. *Cell Biol Int* **21**, 619–633.

Clode, P.L., Stern, R.A. and Marshall, A.T. (2007) Subcellular imaging of isotopically labeled carbon compounds in a biological sample by ion microprobe (NanoSIMS). *Microsc Res Tech* **70**, 220–229.

Cuenca, R.E., Pories, W.J. and Bray, J. (1988) Bromine levels in human serum, urine, hair. *Biol Trace Elem Res* **16**, 151–154.

Dunn, J.H. and Wolk, C.P. (1970) Composition of the cellular envelopes of *Anabaena cylindrica*. *J Bacteriol* **103**, 153–158.

Edelmann, L. (2002) Freeze-dried and resin-embedded biological material is well suited for ultrastructure research. *J Microsc* **207**, 5–26.

Guerquin-Kern, J.L., Wu, T.D., Quintana, C. and Croisy, A. (2005) Progress in analytical imaging of the cell by dynamic secondary ion mass spectrometry (SIMS microscopy). *Biochim Biophys Acta* **1724**, 228–238.

Hallegot, P., Peteranderl, R. and Lechene, C. (2004) In-situ imaging mass spectrometry analysis of melanin granules in the human hair shaft. *J Invest Dermatol* **122**, 381–386.

Hallegot, P., Audinot, J.N. and Migeon, H.N. (2006) Direct NanoSIMS imaging of diffusible elements in surfaced block of cryo-processed biological samples. *Appl Surf Sci* **252**, 6706–6708.

Herrmann, A., Ritz, K., Nunan, N., Clode, P.L., Pett-Ridge, J., Kilburn, M.R., Murphy, D.V., O'Donnell, A.G. *et al.* (2007) Nano-scale secondary ion mass spectrometry – a new analytical tool in biogeochemistry and soil ecology: a review article. *Soil Biol Biochem* **39**, 1835–1850.

Hutber, G.N., Rogers, L.J. and Smith, A.J. (1979) Influence of pesticides on the growth of cyanobacteria. *Z Allg Mikrobiol* **19**, 397–402.

Jancan, S., Trevisan, R. and Paoletti, M.G. (2007) Soil algae composition under different agro-ecosystems in North-Eastern Italy. *Agricult Ecosys Environ* **112**, 1–12.

Krein, A., Audinot, J.N., Migeon, H.N. and Hoffmann, L. (2007) Facing hazardous matter in atmospheric particles with NanoSIMS. *Environ Sci Pollut Res Int* **14**, 3–4.

Laskowski, D.A. (1999) Physical and chemical properties of pyrethroids. *Rev Environ Contam Toxicol* **39**, 1737–1769.

Lechene, C., Hillion, F., McMahon, G., Benson, D., Kleinfeld, A.M., Kampf, J.P., Distel, D., Luyten, I. *et al.* (2006) High-resolution quantitative imaging of mammalian and bacterial cells using stable isotope mass spectrometry. *J Biol* **5**, 20.

Madigan, M.T., Martinko, J.M., Jack, P. and Brock, T.D. (2000) *Brock Biology of Microorganisms*. Berlin: Spektrum, Akademischer Verlag.

Mallison, S.M. and Cannon, R.E. (1984) Effects of pesticides on cyanobacterium *Plectonema boryanum* and cyanophage LPP-1. *Appl Environ Microbiol* **47**, 910–914.

Marino, B., Boon, J.J., Hendriks, E., Horreard, F. and Hillion, F. (2006) Imaging TOF-SIMS and NANOSIMS studies of barite-celestite particles in grounds from paintings by van Gogh. *e-Preservation Science* **3**, 41–50.

Marshall, R.A., Hamilton, J.T., Dring, M.J. and Harper, D.B. (2003) Do vesicle cells of the red alga *Asparagopsis* (Falkenbergia stage) play a role in bromocarbon production? *Chemosphere* **52**, 471–475.

Marxer, C.G., Kraft, M.L., Weber, P.K., Hutcheon, I.D. and Boxer, S.G. (2005) Supported membrane composition analysis by secondary ion mass spectrometry with high lateral resolution. *Biophys J*, **88**, 2965–2975.

McMahon, G., Glassner, B.J. and Lechene, C. (2006) Quantitative imaging of cells with multi-isotope imaging mass spectrometry (MIMS) – nanoautography with stable isotope tracers. *Appl Surf Sci* **252**, 6895–6906.

Michelangeli, F., Robson, M.J., East, J.M. and Lee, A.G. (1990) The conformation of pyrethroids bound to lipid bilayers. *Biochim Biophys Acta* **1028**, 49–57.

Norland, S., Fagerbakke, K.M. and Heldal, M. (1995) Light element analysis of individual bacteria by X-ray microanalysis. *Appl Environ Microbiol* **61**, 1357–1362.

Parikh, A., Shah, V. and Madamwar, D. (2006) Cyanobacterial flora from polluted industrial effluents. *Environ Monit Assess* **116**, 91–102.

Peteranderl, R. and Lechene, C. (2004) Measure of carbon and nitrogen stable isotope ratios in cultured cells. *J Am Soc Mass Spectrom* **15**, 478–485.

Popa, R., Weber, P.K., Pett-Ridge, J., Finzi, J.A., Fallon, S.J., Hutcheon, I.D., Nealson, K.H. and Capone, D.G. (2007) Carbon and nitrogen fixation and metabolite exchange in and between individual cells of *Anabaena oscillarioides*. *ISME J* **1**, 354–360.

Quintana, C., Bellefqih, S., Laval, J.Y., Guerquin-Kern, J.L., Wu, T.D., Avila, J., Ferrer, I., Arranz, R. *et al.* (2006) Study of the localization of iron, ferritin, and hemosiderin in Alzheimer's disease hippocampus by analytical microscopy at the subcellular level. *J Struct Biol* **153**, 42–54.

Quintana, C., Wu, T.D., Delatour, B., Dhenain, M. and Guerquin-Kern, J.L. (2007) Morphological and chemical studies of pathological human and mice brain at the subcellular level: correlation between light, electron and NanoSIMS Microscopies. *Microsc Res Tech* **70**, 281–295.

Rippka, R. (1988) Isolation and purification of cyanobacteria. *Methods Enzymol* **167**, 3–27.

Rutherford online (2006) Internet: http://www.uniterra.de/rutherford/ele035.htm (acessed July 5, 2007).

Slodzian, G., Daigne, B., Girard, F., Boust, F. and Hillion, F. (1990) Parallel mapping of several elements or isotopes by scanning with a submicron ion probe: first results. *Acad Sci* **311**, 57–64.

Stewart, M., Somlyo, A.P., Somlyo, A.V., Shuman, H., Lindsay, J.A. and Murrell, W.G. (1981) Scanning electron probe x-ray microanalysis of elemental distributions in freeze-dried cryosections of *Bacillus coagulans* spores. *J Bacteriol* **147**, 670–674.

Warley, A. (2006) Is analysis of biological materials with nm spatial resolution possible? *J Phys* **26**, 37–41.

Wehner, R. and Gehring, W. (1995) *Zoologie*. Stuttgart, New York: Thieme.

Widenfalk, A., Svensson, J.M. and Goedkoop, W. (2004) Effects of the pesticides captan, deltamethrin, isoproturon, and pirimicarb on the microbial community of a freshwater sediment. *Environ Toxicol Chem* **23**, 1920–1927.

Wolk, C.P. (1996) Heterocyst formation. *Annu Rev Genet* **30**, 59–78.

Yang, F.H. (2007) Microwave-assisted digestion with atomic absorption spectrometry for determination of Pb, Cd, Cu, Fe, Zn and Mn in food and assessment of uncertainty of analytical results. *Guang Pu Xue Yu Guang Pu Fen Xi* **27**, 1440–1443.